Published in final edited form as:
J Immunol. 2014 May 15; 192(10): 4497–4509. doi:10.4049/jimmunol.1301234.

The Very Low Density Lipoprotein Receptor Attenuates House Dust Mite-induced Airway Inflammation by Suppressing Dendritic Cell-mediated Adaptive Immune Responses

Karin Fredriksson[*,II], **Amarjit Mishra**[*,II], **Jonathan K. Lam**[*,II], **Elizabeth M. Mushaben**[*,II], **Rosemarie A. Cuento**[*], **Katharine S. Meyer**[*], **Xianglan Yao**[*], **Karen J. Keeran**[†], **Gayle Z. Nugent**[†], **Xuan Qu**[‡], **Zu-Xi Yu**[‡], **Yanqin Yang**[§], **Nalini Raghavachari**[§], **Pradeep K. Dagur**[¶], **J. Philip McCoy**[¶], and **Stewart J. Levine**[*]

[*]Laboratory of Asthma and Lung Inflammation, Cardiovascular and Pulmonary Branch, Division of Intramural Research, NHLBI, NIH

[†]Laboratory of Animal Surgery and Resources Core Facility, Division of Intramural Research, NHLBI, NIH

[‡]Pathology Core Facility, Division of Intramural Research, NHLBI, NIH

[§]DNA Sequencing and Genomics Core Facility, Division of Intramural Research, NHLBI, NIH

[¶]Flow Cytometry Core Facility, Division of Intramural Research, NHLBI, NIH

Abstract

The very low density lipoprotein receptor (VLDLR) is a member of the low density lipoprotein receptor family that binds multiple ligands and plays a key role in brain development. Although the VLDLR mediates pleiotropic biological processes, only a limited amount of information is available regarding its role in adaptive immunity. Here, we identify an important role for the VLDLR in attenuating house dust mite (HDM)-induced airway inflammation in experimental murine asthma. We show that HDM-challenged *Vldlr*$^{-/-}$ mice have augmented eosinophilic and lymphocytic airway inflammation with increases in Th2 cytokines, C-C chemokines, IgE production and mucous cell metaplasia. A genome-wide analysis of the lung transcriptome identified that mRNA levels of CD209e (DC-SIGNR4), a murine homologue of DC-SIGN, were increased in the lungs of HDM-challenged *Vldlr*$^{-/-}$ mice, which suggested that the VLDLR might modify dendritic cell (DC) function. Consistent with this, VLDLR expression by human monocyte-derived DCs was increased by HDM stimulation. In addition, 55% of peripheral blood CD11c^{+} DCs from individuals with allergy expressed VLDLR under basal conditions. Lastly, the adoptive transfer of HDM-pulsed, CD11c^{+} bone marrow-derived DCs (BMDCs) from *Vldlr*$^{-/-}$ mice to the airways of wild type (WT) recipient mice induced augmented eosinophilic and lymphocytic airway inflammation upon HDM challenge with increases in Th2 cytokines, C-C chemokines, IgE production and mucous cell metaplasia, as compared to the adoptive transfer of HDM-pulsed, CD11c^{+} BMDCs from WT mice. Collectively, these results identify a novel role for

Corresponding Author: Stewart J. Levine, Cardiovascular and Pulmonary Branch, National Heart, Lung, and Blood Institute, National Institutes of Health, Building 10, Room 6D03, MSC 1590, Bethesda, Maryland 20892-1590, Tel. 301-402-1448; Fax. 301-451-5633; levines@nhlbi.nih.gov.
[II]These authors contributed equally to this work.

the VLDLR as a negative regulator of DC-mediated adaptive immune responses in HDM-induced allergic airway inflammation.

Introduction

The low density lipoprotein (LDL) receptor plays a key role in lipid metabolism by facilitating the transport of cholesterol into cells via receptor-mediated endocytosis (1). The LDL receptor is also expressed by ciliated airway epithelial cells in the lung where it negatively regulates house dust mite (HDM)-induced airway hyperresponsiveness (AHR) and mucous cell metaplasia in experimental murine asthma by binding to apolipoprotein E, which is expressed by alveolar macrophages (2). Apolipoprotein E can bind to all seven members of the LDL receptor family, including the widely expressed very low density lipoprotein receptor (VLDLR)(3). The structure of the VLDLR is characterized by an extracellular domain comprised of eight cysteine-rich ligand-binding repeats, an epidermal growth factor domain, an O-linked glycosylated domain, a transmembrane domain and an intracytoplasmic domain that contains a NPxY motif (4, 5). Similar to the LDL receptor, the VLDLR binds and internalizes triglyceride-rich lipoproteins that are enriched for apolipoprotein E, as well as those that have been catabolized by lipoprotein lipase (6).

The VLDLR is a multi-ligand receptor that mediates pleiotropic biological processes. The VLDLR, together with the apolipoprotein receptor 2 (APOER2), function as a heterodimeric receptor for the oligomeric form of reelin, which is a large extracellular matrix protein that is expressed in the embryonal brain and regulates central nervous system development by directing neuronal migration (3, 4, 7). Both the VLDLR and the APOER2 are required to bind oligomeric reelin in the brain (4, 7–9). This activates cellular signaling pathways via the cytoplasmic adaptor protein, disabled-1, which binds to the NPxY motif in the intracytoplasmic domains of VLDLR and APOER2. Consistent with its important role in neural development, mutations in the VLDLR gene have been associated with severe central nervous system developmental disorders in humans, such as cerebellar hypoplasia, quadrapedal locomotion, and disequilibrium syndrome (10, 11). Mice with targeted deletions of the *Vldlr* gene similarly have defects in neuronal migration (9).

In contrast to its central role in neuronal development, only a limited amount of information is available regarding the involvement of the VLDLR in inflammatory or immune responses. Signaling of apolipoprotein E via the VLDLR in macrophages has been reported to promote differentiation to a M2 phenotype characterized by the production of IL-13 and IL-1RA(12). This could be relevant for asthma pathogenesis as IL-13 is a canonical Th2 cytokine that plays an important role in mediating eosinophilic airway inflammation, mucous cell metaplasia, airway fibrosis and AHR(13). Binding of reelin to VLDLR on macrophages also induced expression of the *Pla2g7* gene and promoted production of platelet-activating factor acetylhydrolase (PAFAH), which increased PAFAH secretion into mother's milk and suppressed systemic inflammation in nursing newborns (14). PAFAH catalyzes the degradation of platelet-activating factor and variants in the *Plag2g7* gene have been associated with an increased risk of asthma and allergy (15). Endothelial cell VLDLR has also been identified as a fibrin receptor that promotes inflammation by facilitating the fibrin-

dependent transmigration of leukocytes during vascular injury (16). This too may be relevant for asthma pathogenesis as fibrin deposition has been reported along the luminal surface of distal airways in an asthmatic patient and in a murine model of allergic airway inflammation (17).

Since the VLDLR is structurally similar to the LDLR we hypothesized that it might also regulate the pathogenesis of HDM-induced asthma (2, 5). Here, we show that *Vldlr*$^{-/-}$ mice when challenged with HDM, display a phenotype of augmented eosinophilic and lymphocytic airway inflammation with increases in Th2 cytokines, C-C chemokines, IgE production and mucous cell metaplasia. Furthermore, we utilized adoptive transfer experiments to demonstrate that HDM-pulsed CD11c^{+} dendritic cells from *Vldlr*$^{-/-}$ mice have an enhanced ability to induce airway inflammation in recipient mice upon subsequent HDM challenge. These results show that the VLDLR functions as a negative regulator of HDM-induced airway inflammation by attenuating dendritic cell-mediated adaptive immune responses.

Methods

Murine Models of HDM-induced Airway Disease

Vldlr$^{-/-}$ mice and wild type (WT) B6129SF2/J mice were obtained from Jackson Laboratories (Bar Harbor, Maine). Two models of HDM-induced airway disease were utilized. In the first model, 6-to-8 week old *Vldlr*$^{-/-}$ and WT mice received daily intranasal challenges of 25 μg of HDM (*Dermatophagoides pteronyssinus* extract, Greer Laboratories, Lenoir, NC) or saline, both in a volume of 10 μl, five days a week for six weeks and end-points were analyzed on day 43. Each mg of HDM protein, which had not been de-fatted, contained ≤ 50 units of LPS so that ≤ 125 pg of LPS was administered with each dose (18). In the second model, 0.5×10^5 CD11c^{+} bone marrow-derived dendritic cells (BMDCs) from *Vldlr*$^{-/-}$ and WT mice that had been pulsed with HDM (100 μg/ml) or sham-pulsed with PBS were adoptively transferred in 20 ul of PBS via intranasal administration on day 0 to recipient WT mice (19). All recipient mice received daily intranasal HDM challenges (25 μg) on days 11 through 14 and endpoints were analyzed on day 15. Experimental protocols were approved by the Animal Care and Use Committee of the National Heart, Lung and Blood Institute.

Bronchoalveolar Lavage Fluid Cells

Bronchoalveolar lavage was performed three times with 0.5 ml PBS and red blood cells were lysed with ACK buffer for 2 min at 4°C, as previously described (2, 20). BALF cells were re-suspended in 0.3 ml RPMI-1640 containing 10% FBS and cell counts were performed using a hemocytometer, while differential cell counts were performed on Diff-Quik-stained cytospin slides (Siemens, Deerfield, Illinois).

Lung Histopathology

Lungs were inflated with 10% formalin to a pressure of 25 cm H_20, fixed in 10% formalin for 24 h, dehydrated through gradient ethanol, and embedded in paraffin. Sagittal sections were then cut at a thickness of 5 μm and stained with hematoxylin and eosin and periodic

acid Schiff (PAS). Quantification of mucous cell metaplasia was performed as previously described (2). All the airways present (large (conducting), medium (central), and small (distal)) within a representative lung section were inspected. The number of airways that contained PAS-positive cells were counted and mucous cell metaplasia is reported as the percentage of airways that contained PAS-positive cells. The number of airways inspected in each animal is also presented.

Plasma IgE

Levels of plasma IgE were quantified using an ELISA kit from BD Biosciences Pharmingen (San Diego, CA) with a detection limit of 1.6 ng/ml for IgE.

mRNA Analysis

Quantitative real time-polymerase chain reaction (qRT-PCR) was performed as previously described (21). Lungs were minced into 1 mm pieces and stored in RNAlater (Ambion, Austin, TX) at −80°C prior to isolation of total RNA using a lipid tissue kit (Qiagen Inc, Valencia, CA). On-column DNase treatment was performed using RNase-Free DNase from Qiagen prior to reverse transcription utilizing random hexamer primers and High Capacity cDNA Reverse Transcription Kit (Applied Biosystems, Foster City, CA). PCR was performed on 1 μg of cDNA utilizing the TaqMan Universal PCR Master Mix and the following FAM dye-labeled Taqman® MGB probes; IL-4: Mm00445259_m1, IL-13: Mm00434204_m1, IL-17a: Mm00439618_m1, CCL7: Mm00443113_m1, CCL11: Mm00441238_m1, CCL17: Mm00516136_m1, CCL24: Mm00444701_m1 and 18S: Hs99999901_s1. Samples were amplified utilizing the 7500 Real Time PCR System running Sequence Detector version 2.1 software (ABI systems, Foster City, CA) and gene expression was quantified relative to the expression of 18S mRNA using the control sample as a calibrator to calculate the difference in Ct values (ΔΔCt). Results are presented as relative mRNA expression.

HDM Re-stimulation of Mediastinal Lymph Node Cultures and Measurement of Th2 and Th17 Cytokines

Single cell suspensions of mediastinal lymph nodes (MLN) from HDM-challenged mice were prepared by passing disrupted lymph nodes through a 100 μm strainer, as previously described (21). Following lysis of red blood cells using ACK buffer, MLN cells were suspended in RPMI 1640 medium containing 10% fetal calf serum, penicillin (50 units/ml), streptomycin (50 μg/ml), and L-glutamine (2 mM) and 4×10^6 cells per well were cultured in 96-well plates with “U”-shaped bottoms. MLN cells were stimulated with HDM (100 μg/ml) or PBS for 96 hours prior to collection. Cytokine production was analyzed by sandwich ELISAs with limits of sensitivity of 15.6 pg/ml for IL-4, IL-6 and IL-17A, 31.25 pg/ml for IL-5 and TGF-β1, and 62.5 pg/ml for IL-13 (R & D Systems, Minneapolis, MN).

Microarray Hybridization and Data Analysis of the Lung Transcriptome

Biotin-labeled sense targets were prepared from samples of total lung RNA using the Affymetrix Whole-Transcript (WT) Sense Target Labeling Protocol without rRNA reduction. Double-stranded cDNA templates were synthesized from 50 ng of total RNA

using random hexamers coupled with a T7 promoter sequence and amplified by *in vitro* transcription (IVT) with T7 RNA polymerase to produce multiple copies of cRNAs. Random hexamers were utilized to prepare sense strand cDNA. 10 μg of sense strand cDNA was fragmented, labeled with biotin using terminal deoxynucleotidyl transferase, hybridized to Affymetrix Mouse Gene 1.0 ST microarrays at 45°C overnight, followed by washing and staining using a FS450 fluidics station (Affymetrix, Santa Clara, CA). Scanning was performed using the 7G GCS3000 scanner and gene-level intensity values for each of the chips were collected using Affymetrix Expression Console (EC) Software (Affymetrix, Santa Clara, CA). Raw data pre-processing that included global background correction, quantile normalization and median polish summarization, was performed using the RMA-sketch workflow. Principal component analysis was performed for detecting outliers across all chips. The comparison between HDM-challenged *Vldlr*$^{-/-}$ and wild type groups were assessed using a one-way ANOVA implemented in the MSCL Analyst's Toolbox (http://abs.cit.nih.gov/MSCLtoolbox/) and JMP statistical software package (SAS, Inc, http://www.jmp.com). Differentially expressed genes were selected using the following filters; fold change greater than two and P value less than 0.001 (20%FDR). The data discussed in this publication have been deposited in NCBI's Gene Expression Omnibus and are accessible through GEO Series accession number GSE55247 (http://www.ncbi.nlm.nih.gov/geo/query/acc.cgi?acc=GSE55247)(22).

Generation and Characterization of Murine Bone Marrow-derived Dendritic Cells (BMDCs) and Human Monocyte-derived Dendritic Cells (moDCs)

Bone marrow cells that had been isolated from WT and *Vldlr*$^{-/-}$ mice were cultured at a density of 2×10^6 cells/ml in RPMI 1640 medium (Gibco/Life Technologies, Carlsbad, CA) supplemented with 10% heat-inactivated FCS, penicillin (100 U/ml), streptomycin (100 μg/ml), L-glutamine (2 mM), 2-mercaptoethanol (50 μM), and recombinant mouse GM-CSF (20 ng/ml) (BioLegend, San Diego, CA)(23). An equal volume of medium was added on day 3 and 50% of the medium was replaced on day 6. On day 8, floating cells were collected and viable CD11c$^+$ bone marrow-derived dendritic cells (BMDCs) were sorted by flow cytometry and stimulated with HDM (100 μg/ml) or PBS for 16 h. CD11c$^+$ BMDCs were then utilized for adoptive transfer experiments or analyzed for cell surface marker expression. BMDCs were washed in PBS containing 1 mM EDTA and 10% mouse serum (Jackson ImmunoResearch, Inc., West Grove, PA) and reacted with 5 μg/ml of anti-mouse CD11c-APC-Cy7, CD80-PE-Cy5, CD86-eFluor 605 NC, or CD209-eFluor 660 (eBiosciences, San Diego, CA), followed by two additional washes. Data were acquired on a LSRII (BD Biosciences, USA) equipped with 407, 488, 532, and 633 LASER lines using DIVA 6.1.2 software and analyzed with the Flow Jo software version 9.6.1 (Treestar, San Carlos, CA). Cellular debris was excluded using a forward light scatter/side scatter plot.

Elutriated human monocytes that were provided under an IRB-approved protocol by the NIH Department of Transfusion Medicine, Clinical Center, were cultured in 10 cm petri dishes (BD Biosciences, San Jose, CA) in RPMI 1640 containing 10% FBS, L-glutamine (2 mM), penicillin (100 U/ml), and streptomycin (100 μg/ml) (Gibco/Life Technologies), which had been supplemented with human recombinant GM-CSF (150 ng/ml) and IL-4 (25 ng/ml) (BioLegend, San Diego, CA). On day 7, cells were stimulated with HDM (100

μg/ml) for 16 hours. Human monocyte-derived dendritic cells (moDCs) were then reacted with 5 μg/ml of anti-human CD 11c- Brilliant Violet 711, anti-human CD14-Alexa Fluor 488, anti-human HLA-DR-PerCP/Cy5.5 (Biolegend, San Diego, CA) and rabbit anti-VLDLR-PE-Cy5.5 (Bioss, Inc., MA). Flow cytometry was performed as described above.

Characterization of Peripheral Blood Dendritic Cells from Human Subjects

Informed consent was obtained from 23 volunteers, as per protocol 99-H-0076, which was approved by the Institutional Review Board of the National Heart, Lung, and Blood Institute. Allergy skin testing was performed using a Multi-Test II® applicator (Lincoln Diagnostics, Decatur, IL) with glycerin as a negative control and histamine as a positive control (Holister-Stier, Spokane, WA). Allergy was defined by the presence of skin test reactivity to at least one of six common aeroallergens, which included house dust mite (*Dermatophagoides farinae*), cockroaches (*P. Americana* and *B. germanica*), cat hair, *Aspergillus fumigatus*, Ragweed (Giant and Short) and grasses (Kentucky Bluegrass, Orchard, Redtop, Timothy, Sweet Vernalgrass, Meadow Fescue and Perennial Ryegrass). Individuals without allergy were defined by the absence of a history of allergy and negative skin tests to the six common aeroallergens. Peripheral blood was collected in 10 ml sodium heparinized vacutainers (Becton Dickinson, Franklin Lakes, NJ) and red blood cells were lysed using ACK lysing buffer. Peripheral blood cells were then reacted with anti-human CD11c-APC-Cy7 (clone Bu15), anti-human CD14-Alexa Fluor 488 (clone HCD14), anti-human HLA-DR-PE (clone L243), anti-human CD209-APC (clone 9E9A8), all from Biolegend (San Diego, CA), and rabbit anti-VLDLR-PE-Cy5.5 from Bioss (Woburn, MA) in the presence of 1% normal mouse serum for 45 min in the dark at room temperature. Samples were washed and stained with a fixable live/dead stain (Fixable Viability Dye eFlour® 450, eBioscience, San Diego, CA) for 5 min at room temperature, followed by additional washes and fixation with 1% paraformaldehyde. Data were acquired on a LSRII flow cytometer (BD Biosciences, USA) equipped with 407, 488, 532, and 633 LASER lines using DIVA 6.1.2 software and analyzed with the Flow Jo software version 9.6.4 (Treestar, San Carlos, CA). Cellular debris was excluded using a forward light scatter/side scatter plot. Cell surface expression of VLDLR and CD209 were analyzed on viable $CD11c^{+}/CD14^{-}/HLA\text{-}DR^{+}$ cells. Positive staining for VLDLR was determined using florescence minus one (FMO) for the VLDLR antibody as the control for samples from each individual.

Characterization of VLDLR Expression by Dendritic Cell Subsets in the Lungs and Mediastinal Lymph Nodes of Wild Type Mice

Lung and MLN cells were isolated from saline- and HDM-challenged WT mice by enzymatic digestion with liberase (100 ug/ml) (Roche, Indianapolis, IN) and DNase I (0.2 mg/ml)(Sigma-Aldrich, St. Louis, MO) while agitated at 37° C for 25 min. Single cell suspensions were reacted with the following anti-mouse antibodies in the presence of 1% mouse serum for 30 min at RT in the dark; CD11c-APC-780, MHC-II-PE-CY7, Mar-1-eFluor® 450, CD103-APC, and PDCA-1-Alexa Fluor® 488, all from eBiosciences (San Diego, CA), as well as CD11b-Brilliant Violet 605 and CD64-PerCP-Cy5.5, both from Biolegend (San Diego, CA). The anti-rat VLDLR antibody (6A6, Santa Cruz Biotechnology, Santa Cruz, CA) that recognizes mouse VLDLR was conjugated with PE using a Zenon® labeling kit (Invitrogen, Carlsbad, CA). Following two washes, data was

acquired on a LSRII (BD Biosciences, USA) flow cytometer equipped with 407, 488, 532, and 633 LASER lines using DIVA 6.1.2 software and analyzed with Flow Jo software version 9.6.4 (Treestar, San Carlos, CA). Positive staining for VLDLR was again determined using florescence minus one (FMO) for the VLDLR antibody as the control.

Statistics

Data were analyzed using GraphPad Prism version 5.0a and are presented as mean ± SEM. A one-way ANOVA with Bonferroni's multiple comparison test or a Student's t test for comparison of two groups were used for the analyses. A P value < 0.05 was considered significant.

Results

House dust mite-induced Airway Inflammation and Mucous Cell Metaplasia are Augmented in *Vldlr*$^{-/-}$ mice

Multiple nasal HDM challenges were administered, 5 days per week for 6 weeks, to WT and *Vldlr*$^{-/-}$ mice in order to assess whether the VLDLR modifies the pathogenesis of experimental asthma (Figure 1A). As shown in Figure 1B, there was augmented airway inflammation with significant increases in the total number of bronchoalveolar lavage fluid (BALF) cells in HDM-challenged *Vldlr*$^{-/-}$ mice as compared to WT mice. Furthermore, the increase in BALF cells from HDM challenged *Vldlr*$^{-/-}$ mice represented eosinophils and lymphocytes, whereas there were no differences in the numbers of alveolar macrophages or neutrophils (Figure 1C). Similarly, lung histology revealed an increase in peri-bronchial inflammatory cell infiltrates in HDM-challenged *Vldlr*$^{-/-}$ mice as compared to WT mice (Figure 2A). HDM-challenged *Vldlr*$^{-/-}$ mice also had a significant increase in mucous cell metaplasia as compared to HDM-challenged WT mice (Figure 2A and B). Lastly, neither the WT B6129SF2/J mice nor the *Vldlr*$^{-/-}$ mice developed AHR to nebulized methacholine (not shown), which likely is a result of the genetic background of this mouse strain.

Production of IgE, Th2 Cytokines and C-C Chemokines are Increased in House Dust Mite-challenged *Vldlr*$^{-/-}$ mice

Additional experiments were conducted to characterize further the effects of the VLDLR on the manifestations of HDM-induced airway inflammation. First, plasma IgE levels were markedly increased in HDM-challenged *Vldlr*$^{-/-}$ mice as compared to HDM-challenged wild type mice (Figure 2C). Next, we assessed whether the increases in BALF eosinophils and lymphocytes were associated with the increased expression of Th2 cytokines. As shown in Figure 3A, mRNA levels of Th2 cytokines, IL-4 and IL-13, were significantly increased in the lungs of HDM-challenged *Vldlr*$^{-/-}$ mice, whereas IL-17A mRNA levels were not different as compared to HDM-challenged WT mice. The increase in lung Th2 cytokine production by HDM-challenged *Vldlr*$^{-/-}$ mice was confirmed by *ex vivo* re-stimulation experiments using mediastinal lymph node (MLN) cells from HDM-challenged mice. As shown in Figure 3B, the secretion of the Th2 cytokines, IL-4, IL-5 and IL-13, by T cells present in MLN cultures from HDM-challenged *Vldlr*$^{-/-}$ mice in response to HDM re-stimulation were significantly increased as compared to those from WT mice. In contrast, there was no difference in IL-17A secretion. This demonstrates that Th2 responses are

augmented in HDM-challenged *Vldlr*$^{-/-}$ mice, whereas Th17 responses are not modified. Similarly, lung mRNA levels of C-C chemokines, such as CCL7, CCL11 and CCL24, which mediate eosinophil chemotaxis were significantly increased in the lungs of HDM-challenged *Vldlr*$^{-/-}$ mice (Figure 4). Lung mRNA levels of the C-C chemokine, CCL17, which facilitates the recruitment of Th2 cells, were likewise increased in HDM-challenged *Vldlr*$^{-/-}$ mice.

Expression Profiling of the Lung Transcriptome Identifies Increased Expression of CD209e (DC-SIGNR4) in HDM-challenged *Vldlr*$^{-/-}$ mice

A genome-wide analysis of the lung transcriptome was performed to investigate the mechanism by which the enhanced Th2-mediated airway inflammation was mediated in HDM-challenged *Vldlr*$^{-/-}$ mice. As shown in Figure 5A, the gene that had the highest level of expression in the lungs of HDM-challenged *Vldlr*$^{-/-}$ mice as compared to HDM-challenged wild type mice was CD209e (DC-SIGN-related protein 4, DC-SIGNR4), which is a murine homologue of human CD209, also known as DC-SIGN. Other differentially expressed genes are shown in Supplemental Figure 1. The increased expression of CD209e mRNA in the lungs of HDM-challenged *Vldlr*$^{-/-}$ mice as compared to HDM-challenged WT mice was confirmed by qRT-PCR (Figure 5B).

Since human DC-SIGN is primarily expressed by dendritic cells (DCs), we hypothesized the VLDLR expression by DCs might attenuate Th2 responses during HDM-induced airway inflammation (24, 25). To test this hypothesis, we first assessed whether the VLDR is expressed by human DCs. To demonstrate this, flow cytometry was performed on human monocyte-derived CD11c^{+}/CD14^{-}/HLA-DR^{+} dendritic cells (moDCs), which showed that a subset of moDCs express VLDLR in response to HDM stimulation (Figure 5C – E). We then investigated whether DCs present in peripheral blood samples from a cohort of individuals with and without allergy express VLDLR. As shown in Figure 6A – B, individuals with positive skin test reactivity to at least one of 6 common aeroallergens had significantly higher serum IgE levels than those without allergy, whereas there was no difference in the number of peripheral blood eosinophils between the two groups. There were also no differences in the percentage of CD11c^{+}/CD14^{-}/HLA-DR^{+}/VLDLR^{+} (54.5% ± 5.7% vs. 50.75% ± 5.3%) or CD11c^{+}/CD14^{-}/HLA-DR^{+}/VLDLR^{+}/CD209^{+} (10.5% ± 2.2% vs. 8.9% ± 3.1%) peripheral blood DCs from allergic as compared to non-allergic individuals (Figure 6D and 6E). Collectively, these results show that the VLDLR is expressed on the surface of human peripheral blood DCs under basal conditions and that a subset co-express CD209.

Next, we investigated which DC subtypes in the lung and MLNs of WT mice express the VLDLR and whether VLDLR expression can be induced by HDM. As shown in Figure 7, CD11b^{+} monocyte-derived DCs (moDCs) had the highest percentage of VLDLR^{+} cells in the lungs of saline-challenged mice, whereas very few conventional myeloid CD11b^{+} DCs (CD11b^{+} cDCs) and none of the CD11b^{-} DCs, such as CD103^{+} DCs or plasmacytoid DCs (pDCs), demonstrated VLDLR expression. Following multiple HDM challenges, the percentage of VLDLR^{+} CD11b^{+} cDCs, CD103^{+} DCs and pDCs in the lung were increased. Similarly, moDCs had the highest percentage of VLDLR^{+} cells in the MLNs of saline-

challenged mice and there were significant increases in the percentage of VLDLR$^+$ moDCs, CD11b$^+$ cDCs and pDCs following multiple HDM challenges. These data demonstrate that moDCs have the highest percentage of VLDLR$^+$ cells in the lungs and MLNs of WT mice and that the number of DCs that express the VLDLR can be increased in response to HDM challenge.

Adoptive Transfer of HDM-pulsed CD11c$^+$ Bone Marrow-derived Dendritic Cells Augments Airway Inflammation in HDM-challenged Recipient Mice

Next, adoptive transfer experiments of CD11c$^+$ bone marrow-derived dendritic cells (BMDCs) were performed to assess whether the increased HDM-induced airway inflammation in *Vldlr*$^{-/-}$ mice reflected an enhanced ability of DCs to induce an adaptive immune response to HDM. As shown in Figures 8A and 8B, the MFI of CD80 and CD209 expression was higher on HDM-pulsed, CD11c$^+$/MHCII$^+$ BMDCs from *Vldlr*$^{-/-}$ mice as compared to BMDCs from WT mice, whereas the MFI of CD86 expression was not modified. Adoptive transfer of HDM-pulsed, CD11c$^+$ BMDCs from *Vldlr*$^{-/-}$ donor mice to recipient WT mice showed significant increases in the total number of BALF cells, which reflected eosinophils, neutrophils, lymphocytes and alveolar macrophages, in response to daily intranasal HDM challenges for 4 days as compared to recipient mice that received HDM-pulsed, CD11c$^+$ BMDCs from WT donor mice (Figures 8C and 8D). Similarly, mice that received HDM-pulsed, CD11c$^+$ BMDCs from *Vldlr*$^{-/-}$ donor mice had increased peri-bronchial inflammatory cell infiltrates and mucous cell metaplasia on lung histology (Figure 8E and 9A). In addition, mucous cell metaplasia was increased in HDM-challenged mice that received PBS-pulsed CD11c$^+$ BMDCs from *Vldlr*$^{-/-}$ donor mice as compared to recipients of PBS-pulsed CD11c$^+$ BMDCs from WT donor mice (Figures 8E and 9A). Although lung histology also showed peribronchial inflammation in HDM-challenged mice that received PBS-pulsed CD11c$^+$ BMDCs from *Vldlr*$^{-/-}$ donor mice, there was no difference in the number of BALF inflammatory cells when compared to recipients of PBS-pulsed CD11c$^+$ BMDCs from WT donor mice.

HDM re-stimulation of e*x vivo* cultures of MLN cells from mice that had received HDM-pulsed, CD11c$^+$ BMDCs from *Vldlr*$^{-/-}$ donors had significant increases in the production of the Th2 cytokines, IL-4 and IL-5, as compared to recipients that received HDM-pulsed, CD11c$^+$ BMDCs from WT donors, whereas production of IL-13 and IL-17A were not significantly increased (Figure 9B). Consistent with the absence of an effect of HDM-pulsed, CD11c$^+$ BMDCs from *Vldlr*$^{-/-}$ donor mice on Th17 immune responses, BALF levels of TGF-β1 and IL-6, which are key cytokines that induce the differentiation of Th17 cells, were not different between recipients of HDM-pulsed, CD11c$^+$ BMDCs from WT or *Vldlr*$^{-/-}$ donors (Figure 9C & 9D) (26–28). Recipients of HDM-pulsed BMDCs from *Vldlr*$^{-/-}$ donors also had significant increases in BALF levels of the C-C chemokines, CCL17, CCL22 and CCL24 (Figure 9E–G), and plasma IgE (Figure 9H). Thus, the adoptive transfer of HDM-pulsed, CD11c$^+$ BMDCs from *Vldlr*$^{-/-}$ donor mice significantly up-regulated Th2-mediated airway inflammatory responses in WT recipient mice upon subsequent HDM challenge as compared to those that received the adoptive transfer of HDM-pulsed, CD11c$^+$ BMDCs from WT donor mice.

Discussion

The LDL receptor was the first member of the LDL receptor superfamily to be identified to have a role in the pathogenesis of asthma (2). Here, we utilized *Vldlr*$^{-/-}$ mice to assess whether the VLDL receptor, which is another member of the LDL receptor family, also modulates HDM-induced airway disease (29). Although the VLDLR mediates the binding and uptake of very low density lipoproteins, *Vldlr*$^{-/-}$ mice have normal plasma cholesterol, triacylglycerol and lipoprotein levels despite normal or high-fat diets, which demonstrates that the VLDLR is not required for the clearance of VLDL particles from plasma (29). *Vldlr*$^{-/-}$ mice, however, have a modest decrease in adipose tissue mass and are protected from obesity when fed a high-fat, high-calorie diet (29, 30). The VLDLR has recently been shown to promote lipotoxicity and increase mortality related to acute myocardial infarction by reducing ischemia-mediated stress responses in the endoplasmic reticulum of mouse myocytes (31). The VLDLR also promotes atherosclerotic lesion development by facilitating the accumulation of atherogenic lipoproteins in macrophages (32). Lastly, the VLDLR attenuates signaling through the *wnt* pathway, which negatively regulates choroidal neovascularization in age-related macular degeneration (33).

We now show that *Vldlr*$^{-/-}$ mice have a phenotype of augmented airway inflammation and mucous cell metaplasia following sensitization and challenge to the airway by multiple doses of HDM administered over 6 weeks. The amplified eosinophilic and lymphocytic airway inflammation was associated with increases in Th2, but not Th17, responses, in the lung and mediastinal lymph nodes, as well as an increase in plasma IgE production. Similarly, there was increased expression of C-C chemokines, such as CCL7 (MCP-3), CCL11 (eotaxin 1) and CCL24 (eotaxin 2) that mediate the recruitment of eosinophils via CCR3, and CCL17 (TARC), which recruits T cells via CCR4(34, 35). The magnified airway inflammatory responses were associated with significant increases in mucous cell metaplasia. Collectively, these results demonstrate that the VLDL receptor functions to attenuate HDM-induced airway inflammation and mucous cell metaplasia in asthma.

We next hypothesized that the increased airway inflammation in HDM-challenged *Vldlr*$^{-/-}$ mice might be mediated at the level of the dendritic cell based upon a genome-wide analysis of the lung transcriptome that demonstrated increased expression of CD209e (DC-SIGNR4), which is one of eight murine homologues of human CD209 gene (36, 37). Furthermore, CD209e expression is up-regulated in immunological cells recruited to the airways of ovalbumin-challenged mice (38). CD209e shares 70% homology with human DC-SIGN (Dendritic Cell-Specific Intracellular adhesion molecule (ICAM)-3-Grabbing Non-integrin), which is a C-type lectin pattern recognition receptor that is primarily expressed by immature dendritic cells (24, 25, 38). DC-SIGN mediates immune responses to a variety of pathogens, such as viruses, bacteria, yeast and parasites, and was originally identified by its ability to interact with HIV-1 at sites of infection. DC-SIGN has also been found to play a role in immune responses to allergens, including house dust mite. For example, DC-SIGN binds both Der p1 and Der p2, which are major HDM antigens, while Der p1, which is a cysteine protease, cleaves DC-SIGN from human moDCs (39, 40),(41). Studies utilizing moDCs, however, have found conflicting results regarding the role of DC-SIGN in HDM-mediated immune responses. In one study, DC-SIGN activation of immature moDCs by HDM extract

promoted Th2 cytokine production by co-cultured $CD4^+$ T cells, which could be inhibited by an anti-DC-SIGN antibody. This was seen in moDCs from allergic asthmatics, but not in those from non-allergic control subjects. This suggests that DC-SIGN plays an important role in allergen sensitization to HDM by mediating the internalization of HDM antigens, which results in an enhanced ability of mature DCs to promote Th2 polarization of naïve $CD4^+$ T cells (42). Another study, however, showed that down-regulation of DC-SIGN expression on immature human peripheral blood moDCs by RNA interference promoted a Th2 phenotype in T cell co-culture experiments (39).

Previous studies have not addressed whether the VLDLR receptor is expressed by or modifies adaptive immune responses mediated by DCs. Here, we show that a subset of $CD11c^+$/HLA-DR^+ human monocyte-derived dendritic cells (moDCs) express the VLDLR and that *ex vivo* stimulation with HDM increased the percentage of $VLDLR^+$ moDCs. In addition, we show that 54.5% of $CD11c^+$/$CD14^-$/HLA-DR^+ and 10.5% of $CD11c^+$/$CD14^-$/HLA-DR^+/$CD209^+$ peripheral blood DCs from human subjects with documented allergy expressed the VLDLR under basal conditions. Next, we isolated lungs and MLNs from WT mice to characterize VLDLR expression by subsets of $CD11c^{+/}MHCII^+$ DCs, which are key antigen-presenting cells that are required for Th2-mediated airway inflammation in asthma (43). $CD11b^+$ DCs that express IRF4 (interferon regulatory factor 4) are effective at antigen presentation via MHCII and promote helper T cell responses, whereas $CD11b^-$ DCs appear to be specialized for the activation of cytotoxic T cells via MHCI(44). Furthermore, both $CD11b^+$ conventional DCs (cDCs) and monocyte-derived DCs (moDCs) are sufficient to induce sensitization and Th2 immune responses to HDM, whereas moDCs also promote allergic inflammation via the production of pro-inflammatory chemokines (45). Among $CD11b^-$ DCs, contrasting results have been reported regarding the ability of $CD103^+$ DCs to induce allergic sensitization and Th2 immune responses to HDM (45–47), whereas plasmacytoid DCs induce the differentiation of regulatory T cells (T regs) that suppress antigen-specific T cell proliferation (47, 48). Here, we show that moDCs are the DC subset with the highest percentage of $VLDLR^+$ cells in mouse lung and MLNs and that the percentage of DCs that express the VLDLR can be increased in response to HDM.

We next generated HDM-pulsed and sham-pulsed $CD11c^+$ BMDCs from *Vldlr*$^{-/-}$ and WT donor mice for adoptive transfer to WT recipient mice to confirm that VLDLR expression modifies the ability of DCs to induce immune responses to HDM in the lung. Recipients of HDM-pulsed, $CD11c^+$ BMDCs from *Vldlr*$^{-/-}$ donor mice demonstrated augmented airway inflammation upon HDM challenge as compared to HDM-pulsed, $CD11c^+$ BMDCs from WT donor mice. In particular, there were significant increases in the number of BALF eosinophils, lymphocytes, neutrophils and macrophages. Furthermore, the adoptive transfer of HDM-pulsed, $CD11c^+$ BMDCs from *Vldlr*$^{-/-}$ donors induced significant increases in Th2 cytokine production by MLN cells following *ex vivo* re-stimulation with HDM, as well as increases in plasma IgE levels and BALF levels of C-C chemokines, CCL17, CCL22 and CCL24. Thus, the phenotype of HDM-challenged recipient mice that received the adoptive transfer of HDM-pulsed, $CD11c^+$ BMDCs from *Vldlr*$^{-/-}$ donors displayed a similar phenotype as *Vldlr*$^{-/-}$ mice that had been directly sensitized and challenged by multiple intranasal exposures to HDM. Collectively, these results show that the adoptive transfer of

HDM-pulsed, $CD11c^+$ BMDCs from *Vldlr*$^{-/-}$ donors have an augmented ability to induce Th2-type airway inflammation upon subsequent HDM challenge. While these data confirm a regulatory role for VLDLR expression by DCs, our results do not exclude the possibility that other $VLDLR^+$ immune or structural cells may also contribute to this effect. Lastly, while cell surface expression of CD209e was higher on HDM-pulsed, $CD11c^+$ BMDCs from *Vldlr*$^{-/-}$ donors, additional studies will be required to determine if CD209e mediates the enhanced HDM-induced airway inflammation that was seen following the adoptive transfer to recipient mice.

Although we have shown that the VLDLR attenuates the ability of DCs to mediate HDM-induced Th2 immune responses, future studies will be required to identify the relevant VLDLR ligands and downstream signaling pathways in DCs that mediate this effect. In the brain, binding of reelin to its heterodimeric receptor, comprised of VLDLR and ApoER2, induces the phosphorylation and recruitment of the intracellular adaptor protein, disabled-1 (Dab1), via Src family kinases (49, 50). Tyrosine-phosphorylated Dab1 then recruits additional SH2-domain containing proteins, such as the p85 regulatory subunit of phosphatidylinositide-3-kinase (PI3K), NCK adaptor protein 2 (Nck2, Nckβ), the Crk family of adaptor proteins, and suppressor of cytokine signaling (SOCS). Lissencephaly 1 (Lis1) can also be recruited by Dab1 via a SH2-domain-independent interaction. In addition to its key role in mediating reelin signaling, the VLDLR has also been shown to bind a variety of other ligands, including the 39-kDa receptor associated protein, thrombospondin, F-spondin, coagulation factor VIII, lipoprotein lipase, urokinase plasminogen activator/plasminogen activator inhibitor-1 complexes, and serpin proteinase/serpin complexes, including those containing thrombin and tissue plasminogen activator (4, 51–57). Therefore, multiple VLDLR ligands and signaling pathways exist that could potentially regulate DC-mediated Th2 adaptive immune responses to HDM.

In summary, we have utilized a HDM model of experimental asthma to show that *Vldlr*$^{-/-}$ mice display a phenotype of augmented allergic airway inflammation that is characterized by significant increases in Th2 cytokines, C-C chemokines, IgE production and mucous cell metaplasia. These results demonstrate that the VLDL receptor attenuates airway inflammation in experimental HDM-induced asthma. Taken together with our prior finding that the LDL receptor is a negative regulator of HDM-induced mucous cell metaplasia and airway hyperresponsiveness, our data are consistent with the conclusion that LDL receptor family members play an important role in limiting excessive HDM-induced airway disease in experimental murine asthma models (2). Furthermore, we used adoptive transfer experiments to show that the VLDLR reduces HDM-induced airway inflammation by a dendritic cell-dependent mechanism. This identifies a novel role for the VLDL receptor in limiting excessive HDM-induced airway inflammation by suppressing dendritic cell-mediated adaptive immune responses manifested by the increased expression of Th2 cytokines, C-C chemokines, and IgE production.

Supplementary Material

Refer to Web version on PubMed Central for supplementary material.

Acknowledgments

Funding: Division of Intramural Research, National Heart, Lung, and Blood Institute.

We are extremely appreciative of the staff of the NHLBI Laboratory of Animal Medicine and Surgery, whose commitment, professional advice and excellent technical support made this study possible. We thank Drs. Joel Moss and Martha Vaughan for their very helpful discussions.

References

1. Goldstein JL, Brown MS. The LDL receptor. Arterioscler Thromb Vasc Biol. 2009; 29:431–438. [PubMed: 19299327]
2. Yao X, Fredriksson K, Yu ZX, Xu X, Raghavachari N, Keeran KJ, Zywicke GJ, Kwak M, Amar MJ, Remaley AT, Levine SJ. Apolipoprotein E Negatively Regulates House Dust Mite-induced Asthma via a LDL Receptor-mediated Pathway. Am J Respir Crit Care Med. 2010; 182:1228–1238. [PubMed: 20622028]
3. Herz J, Chen Y. Reelin, lipoprotein receptors and synaptic plasticity. Nat Rev Neurosci. 2006; 7:850–859. [PubMed: 17053810]
4. Reddy SS, Connor TE, Weeber EJ, Rebeck W. Similarities and differences in structure, expression, and functions of VLDLR and ApoER2. Mol Neurodegener. 2011; 6:30. [PubMed: 21554715]
5. Takahashi S, Sakai J, Fujino T, Miyamori I, Yamamoto TT. The very low density lipoprotein (VLDL) receptor--a peripheral lipoprotein receptor for remnant lipoproteins into fatty acid active tissues. Mol Cell Biochem. 2003; 248:121–127. [PubMed: 12870663]
6. Takahashi S, Suzuki J, Kohno M, Oida K, Tamai T, Miyabo S, Yamamoto T, Nakai T. Enhancement of the binding of triglyceride-rich lipoproteins to the very low density lipoprotein receptor by apolipoprotein E and lipoprotein lipase. J Biol Chem. 1995; 270:15747–15754. [PubMed: 7797576]
7. Herz J, Chen Y, Masiulis I, Zhou L. Expanding functions of lipoprotein receptors. J Lipid Res. 2009; 50(Suppl):S287–292. [PubMed: 19017612]
8. May P, Bock HH, Herz J. Integration of endocytosis and signal transduction by lipoprotein receptors. Sci STKE. 2003; 2003:PE12. [PubMed: 12671190]
9. Trommsdorff M, Gotthardt M, Hiesberger T, Shelton J, Stockinger W, Nimpf J, Hammer RE, Richardson JA, Herz J. Reeler/Disabled-like disruption of neuronal migration in knockout mice lacking the VLDL receptor and ApoE receptor 2. Cell. 1999; 97:689–701. [PubMed: 10380922]
10. Moheb LA, Tzschach A, Garshasbi M, Kahrizi K, Darvish H, Heshmati Y, Kordi A, Najmabadi H, Ropers HH, Kuss AW. Identification of a nonsense mutation in the very low-density lipoprotein receptor gene (VLDLR) in an Iranian family with dysequilibrium syndrome. Eur J Hum Genet. 2008; 16:270–273. [PubMed: 18043714]
11. Ozcelik T, Akarsu N, Uz E, Caglayan S, Gulsuner S, Onat OE, Tan M, Tan U. Mutations in the very low-density lipoprotein receptor VLDLR cause cerebellar hypoplasia and quadrupedal locomotion in humans. Proc Natl Acad Sci U S A. 2008; 105:4232–4236. [PubMed: 18326629]
12. Baitsch D, Bock HH, Engel T, Telgmann R, Muller-Tidow C, Varga G, Bot M, Herz J, Robenek H, von Eckardstein A, Nofer JR. Apolipoprotein E induces antiinflammatory phenotype in macrophages. Arterioscler Thromb Vasc Biol. 2011; 31:1160–1168. [PubMed: 21350196]
13. Zhu Z, Homer RJ, Wang Z, Chen Q, Geba GP, Wang J, Zhang Y, Elias JA. Pulmonary expression of interleukin-13 causes inflammation, mucus hypersecretion, subepithelial fibrosis, physiologic abnormalities, and eotaxin production. J Clin Invest. 1999; 103:779–788. [PubMed: 10079098]
14. Du Y, Yang M, Wei W, Huynh HD, Herz J, Saghatelian A, Wan Y. Macrophage VLDL receptor promotes PAFAH secretion in mother's milk and suppresses systemic inflammation in nursing neonates. Nat Commun. 2012; 3:1008. [PubMed: 22910354]
15. Kruse S, Mao XQ, Heinzmann A, Blattmann S, Roberts MH, Braun S, Gao PS, Forster J, Kuehr J, Hopkin JM, Shirakawa T, Deichmann KA. The Ile198Thr and Ala379Val variants of plasmatic PAF-acetylhydrolase impair catalytical activities and are associated with atopy and asthma. Am J Hum Genet. 2000; 66:1522–1530. [PubMed: 10733466]

16. Yakovlev S, Mikhailenko I, Cao C, Zhang L, Strickland DK, Medved L. Identification of VLDLR as a novel endothelial cell receptor for fibrin that modulates fibrin-dependent transendothelial migration of leukocytes. Blood. 2012; 119:637–644. [PubMed: 22096238]

17. Wagers SS, Norton RJ, Rinaldi LM, Bates JH, Sobel BE, Irvin CG. Extravascular fibrin, plasminogen activator, plasminogen activator inhibitors, and airway hyperresponsiveness. J Clin Invest. 2004; 114:104–111. [PubMed: 15232617]

18. Yao X, Gao M, Dai C, Meyer KS, Chen J, Keeran KJ, Nugent GZ, Qu X, Yu ZX, Dagur PK, McCoy JP, Levine SJ. Peptidoglycan Recognition Protein 1 Promotes House Dust Mite-Induced Airway Inflammation in Mice. Am J Respir Cell Mol Biol. 2013:902–911. [PubMed: 23808363]

19. Pouliot P, Willart MA, Hammad H, Lambrecht BN. Studying the function of dendritic cells in mouse models of asthma. Methods Mol Biol. 2010; 595:331–349. [PubMed: 19941123]

20. Yao X, Dai C, Fredriksson K, Dagur PK, Mccoy JP, Qu X, Yu ZX, Keeran KJ, Zywicke GJ, Amar MJA, Remaley AT, Levine SJ. 5A, an Apolipoprotein A-I Mimetic Peptide, Attenuates the Induction of House Dust Mite-induced Asthma. Journal of Immunology. 2011; 186:576–583.

21. Fredriksson K, Fielhaber JA, Lam JK, Yao X, Meyer KS, Keeran KJ, Zywicke GJ, Qu X, Yu ZX, Moss J, Kristof AS, Levine SJ. Paradoxical effects of rapamycin on experimental house dust mite-induced asthma. PloS One. 2012; 7:e33984. [PubMed: 22685525]

22. Edgar R, Domrachev M, Lash AE. Gene Expression Omnibus: NCBI gene expression and hybridization array data repository. Nucleic Acids Res. 2002; 30:207–210. [PubMed: 11752295]

23. Lutz MB, Kukutsch N, Ogilvie AL, Rossner S, Koch F, Romani N, Schuler G. An advanced culture method for generating large quantities of highly pure dendritic cells from mouse bone marrow. J Immunol Methods. 1999; 223:77–92. [PubMed: 10037236]

24. Zhou T, Chen Y, Hao L, Zhang Y. DC-SIGN and immunoregulation. Cell Mol Immunol. 2006; 3:279–283. [PubMed: 16978536]

25. van Kooyk Y, Geijtenbeek TB. DC-SIGN: escape mechanism for pathogens. Nature Reviews Immunology. 2003; 3:697–709.

26. Kimura A, Kishimoto T. IL-6: regulator of Treg/Th17 balance. Eur J Immunol. 2010; 40:1830–1835. [PubMed: 20583029]

27. Bettelli E, Carrier Y, Gao W, Korn T, Strom TB, Oukka M, Weiner HL, Kuchroo VK. Reciprocal developmental pathways for the generation of pathogenic effector TH17 and regulatory T cells. Nature. 2006; 441:235–238. [PubMed: 16648838]

28. Mangan PR, Harrington LE, O'Quinn DB, Helms WS, Bullard DC, Elson CO, Hatton RD, Wahl SM, Schoeb TR, Weaver CT. Transforming growth factor-beta induces development of the T(H)17 lineage. Nature. 2006; 441:231–234. [PubMed: 16648837]

29. Frykman PK, Brown MS, Yamamoto T, Goldstein JL, Herz J. Normal plasma lipoproteins and fertility in gene-targeted mice homozygous for a disruption in the gene encoding very low density lipoprotein receptor. Proc Natl Acad Sci U S A. 1995; 92:8453–8457. [PubMed: 7667310]

30. Goudriaan JR, Tacken PJ, Dahlmans VE, Gijbels MJ, van Dijk KW, Havekes LM, Jong MC. Protection from obesity in mice lacking the VLDL receptor. Arterioscler Thromb Vasc Biol. 2001; 21:1488–1493. [PubMed: 11557677]

31. Perman JC, Bostrom P, Lindbom M, Lidberg U, St Ahlman M, Hagg D, Lindskog H, Tang M Scharin, Omerovic E, Mattsson Hulten L, Jeppsson A, Petursson P, Herlitz J, Olivecrona G, Strickland DK, Ekroos K, Olofsson SO, Boren J. The VLDL receptor promotes lipotoxicity and increases mortality in mice following an acute myocardial infarction. J Clin Invest. 2011; 121:2625–2640. [PubMed: 21670500]

32. Eck MV, Oost J, Goudriaan JR, Hoekstra M, Hildebrand RB, Bos IS, van Dijk KW, Van Berkel TJ. Role of the macrophage very-low-density lipoprotein receptor in atherosclerotic lesion development. Atherosclerosis. 2005; 183:230–237. [PubMed: 15979629]

33. Chen Y, Hu Y, Lu K, Flannery JG, Ma JX. Very low density lipoprotein receptor, a negative regulator of the wnt signaling pathway and choroidal neovascularization. J Biol Chem. 2007; 282:34420–34428. [PubMed: 17890782]

34. Barnes PJ. The cytokine network in asthma and chronic obstructive pulmonary disease. J Clin Invest. 2008; 118:3546–3556. [PubMed: 18982161]

35. Shang XZ, Chiu BC, Stolberg V, Lukacs NW, Kunkel SL, Murphy HS, Chensue SW. Eosinophil recruitment in type-2 hypersensitivity pulmonary granulomas: source and contribution of monocyte chemotactic protein-3 (CCL7). Am J Pathol. 2002; 161:257–266. [PubMed: 12107110]
36. Park CG, Takahara K, Umemoto E, Yashima Y, Matsubara K, Matsuda Y, Clausen BE, Inaba K, Steinman RM. Five mouse homologues of the human dendritic cell C-type lectin, DC-SIGN. Int Immunol. 2001; 13:1283–1290. [PubMed: 11581173]
37. Powlesland AS, Ward EM, Sadhu SK, Guo Y, Taylor ME, Drickamer K. Widely divergent biochemical properties of the complete set of mouse DC-SIGN-related proteins. J Biol Chem. 2006; 281:20440–20449. [PubMed: 16682406]
38. Di Valentin E, Crahay C, Garbacki N, Hennuy B, Gueders M, Noel A, Foidart JM, Grooten J, Colige A, Piette J, Cataldo D. New asthma biomarkers: lessons from murine models of acute and chronic asthma. Am J Physiol Lung Cell Mol Physiol. 2009; 296:L185–197. [PubMed: 19028979]
39. Emara M, Royer PJ, Mahdavi J, Shakib F, Ghaemmaghami AM. Retagging identifies dendritic cell-specific intercellular adhesion molecule-3 (ICAM3)-grabbing non-integrin (DC-SIGN) protein as a novel receptor for a major allergen from house dust mite. J Biol Chem. 2012; 287:5756–5763. [PubMed: 22205703]
40. Hsu SC, Chen CH, Tsai SH, Kawasaki H, Hung CH, Chu YT, Chang HW, Zhou Y, Fu J, Plunkett B, Su SN, Vieths S, Lee RT, Lee YC, Huang SK. Functional interaction of common allergens and a C-type lectin receptor, dendritic cell-specific ICAM3-grabbing non-integrin (DC-SIGN), on human dendritic cells. J Biol Chem. 2010; 285:7903–7910. [PubMed: 20080962]
41. Furmonaviciene R, Ghaemmaghami AM, Boyd SE, Jones NS, Bailey K, Willis AC, Sewell HF, Mitchell DA, Shakib F. The protease allergen Der p 1 cleaves cell surface DC-SIGN and DC-SIGNR: experimental analysis of in silico substrate identification and implications in allergic responses. Clinical and Experimental Allergy. 2007; 37:231–242. [PubMed: 17250696]
42. Huang HJ, Lin YL, Liu CF, Kao HF, Wang JY. Mite allergen decreases DC-SIGN expression and modulates human dendritic cell differentiation and function in allergic asthma. Mucosal Immunol. 2011; 4:519–527. [PubMed: 21471959]
43. van Rijt LS, Jung S, Kleinjan A, Vos N, Willart M, Duez C, Hoogsteden HC, Lambrecht BN. In vivo depletion of lung CD11c+ dendritic cells during allergen challenge abrogates the characteristic features of asthma. J Exp Med. 2005; 201:981–991. [PubMed: 15781587]
44. Vander Lugt B, Khan AA, Hackney JA, Agrawal S, Lesch J, Zhou M, Lee WP, Park S, Xu M, Devoss J, Spooner CJ, Chalouni C, Delamarre L, Mellman I, Singh H. Transcriptional programming of dendritic cells for enhanced MHC class II antigen presentation. Nat Immunol. 2014; 15:161–167. [PubMed: 24362890]
45. Plantinga M, Guilliams M, Vanheerswynghels M, Deswarte K, Branco-Madeira F, Toussaint W, Vanhoutte L, Neyt K, Killeen N, Malissen B, Hammad H, Lambrecht BN. Conventional and monocyte-derived CD11b(+) dendritic cells initiate and maintain T helper 2 cell-mediated immunity to house dust mite allergen. Immunity. 2013; 38:322–335. [PubMed: 23352232]
46. Mesnil C, Sabatel CM, Marichal T, Toussaint M, Cataldo D, Drion PV, Lekeux P, Bureau F, Desmet CJ. Resident CD11b(+)Ly6C(−) lung dendritic cells are responsible for allergic airway sensitization to house dust mite in mice. PLoS One. 2012; 7:e53242. [PubMed: 23300898]
47. Nakano H, Free ME, Whitehead GS, Maruoka S, Wilson RH, Nakano K, Cook DN. Pulmonary CD103(+) dendritic cells prime Th2 responses to inhaled allergens. Mucosal Immunol. 2012; 5:53–65. [PubMed: 22012243]
48. de Heer HJ, Hammad H, Soullie T, Hijdra D, Vos N, Willart MA, Hoogsteden HC, Lambrecht BN. Essential role of lung plasmacytoid dendritic cells in preventing asthmatic reactions to harmless inhaled antigen. J Exp Med. 2004; 200:89–98. [PubMed: 15238608]
49. Gao Z, Godbout R. Reelin-Disabled-1 signaling in neuronal migration: splicing takes the stage. Cell Mol Life Sci. 2013; 70:2319–2329. [PubMed: 23052211]
50. Gao Z, Poon HY, Li L, Li X, Palmesino E, Glubrecht DD, Colwill K, Dutta I, Kania A, Pawson T, Godbout R. Splice-mediated motif switching regulates disabled-1 phosphorylation and SH2 domain interactions. Mol Cell Biol. 2012; 32:2794–2808. [PubMed: 22586277]
51. Ananyeva NM, Makogonenko YM, Kouiavskaia DV, Ruiz J, Limburg V, Meijer AB, Khrenov AV, Shima M, Strickland DK, Saenko EL. The binding sites for the very low density lipoprotein

receptor and low-density lipoprotein receptor-related protein are shared within coagulation factor VIII. Blood Coagulation & Fibrinolysis. 2008; 19:166–177. [PubMed: 18277139]

52. Argraves KM, Battey FD, MacCalman CD, McCrae KR, Gafvels M, Kozarsky KF, Chappell DA, Strauss JF 3rd, Strickland DK. The very low density lipoprotein receptor mediates the cellular catabolism of lipoprotein lipase and urokinase-plasminogen activator inhibitor type I complexes. J Biol Chem. 1995; 270:26550–26557. [PubMed: 7592875]
53. Battey FD, Gafvels ME, FitzGerald DJ, Argraves WS, Chappell DA, Strauss JF 3rd, Strickland DK. The 39-kDa receptor-associated protein regulates ligand binding by the very low density lipoprotein receptor. J Biol Chem. 1994; 269:23268–23273. [PubMed: 8083232]
54. Blake SM, Strasser V, Andrade N, Duit S, Hofbauer R, Schneider WJ, Nimpf J. Thrombospondin-1 binds to ApoER2 and VLDL receptor and functions in postnatal neuronal migration. The EMBO Journal. 2008; 27:3069–3080. [PubMed: 18946489]
55. Heegaard CW, Simonsen AC, Oka K, Kjoller L, Christensen A, Madsen B, Ellgaard L, Chan L, Andreasen PA. Very low density lipoprotein receptor binds and mediates endocytosis of urokinase-type plasminogen activator-type-1 plasminogen activator inhibitor complex. J Biol Chem. 1995; 270:20855–20861. [PubMed: 7657671]
56. Hoe HS, Wessner D, Beffert U, Becker AG, Matsuoka Y, Rebeck GW. F-spondin interaction with the apolipoprotein E receptor ApoEr2 affects processing of amyloid precursor protein. Mol Cell Biol. 2005; 25:9259–9268. [PubMed: 16227578]
57. Kasza A, Petersen HH, Heegaard CW, Oka K, Christensen A, Dubin A, Chan L, Andreasen PA. Specificity of serine proteinase/serpin complex binding to very-low-density lipoprotein receptor and alpha2-macroglobulin receptor/low-density-lipoprotein-receptor-related protein. European Journal of Biochemistry. 1997; 248:270–281. [PubMed: 9346278]

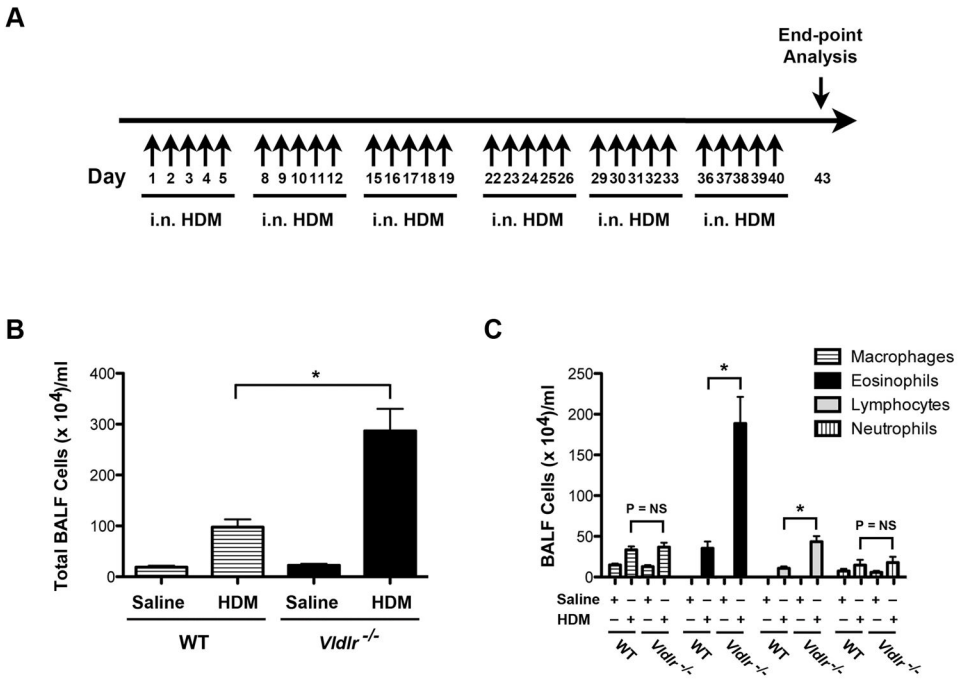

Figure 1. Eosinophilic and lymphocytic airway inflammation are augmented in house dust mite (HDM)-challenged *Vldlr*$^{-/-}$ mice

A. HDM challenge model of experimental asthma. *Vldlr*$^{-/-}$ or wild type mice received daily intranasal challenges of HDM (25 μg in 10 ul saline) or saline alone, 5 days per week, for 6 weeks. End-points were analyzed 72 hours after the last challenge. **B and C**. The number of total bronchoalveolar (BALF) inflammatory cells (Panel B) and inflammatory cell types (Panel C) are shown (n = 18 – 20 mice, *P < 0.0001, *Vldlr* $^{-/-}$ + HDM vs. WT + HDM).

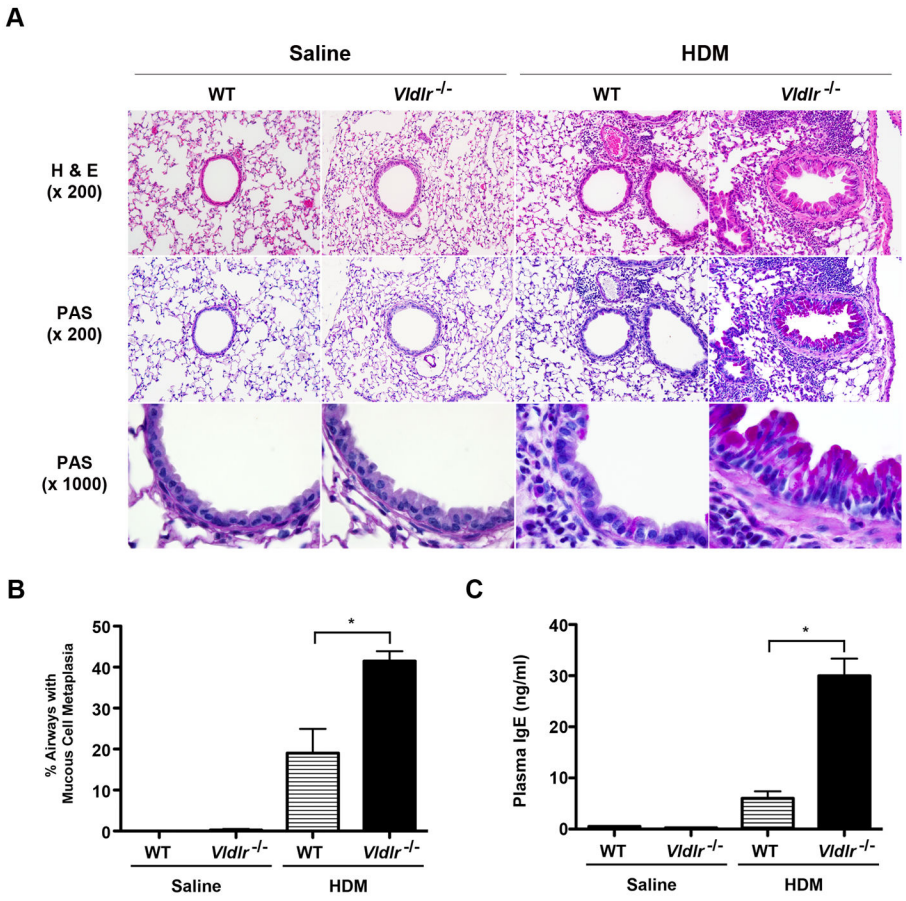

Figure 2. Mucous cell metaplasia and IgE production are augmented in house dust mite (HDM)-challenged *Vldlr*$^{-/-}$ mice

A. Representative histologic sections of lungs from WT and *Vldlr*$^{-/-}$ mice that had been challenged with HDM or saline were stained with hematoxylin and eosin (H & E) (x 200) or periodic acid Schiff (x200 and x1000). **B**. Mucous cell metaplasia is presented as the percentage of airways on lung histological sections that contained periodic acid–Schiff positive cells (n = 10 mice, *P < 0.0001, *Vldlr*$^{-/-}$ + HDM vs. WT + HDM). 35.2 ± 1.7 airways were counted per mouse. **C.** Quantification of plasma IgE levels (n = 19 – 20 mice, *P < 0.0001 *Vldlr*$^{-/-}$ + HDM vs. WT + HDM).

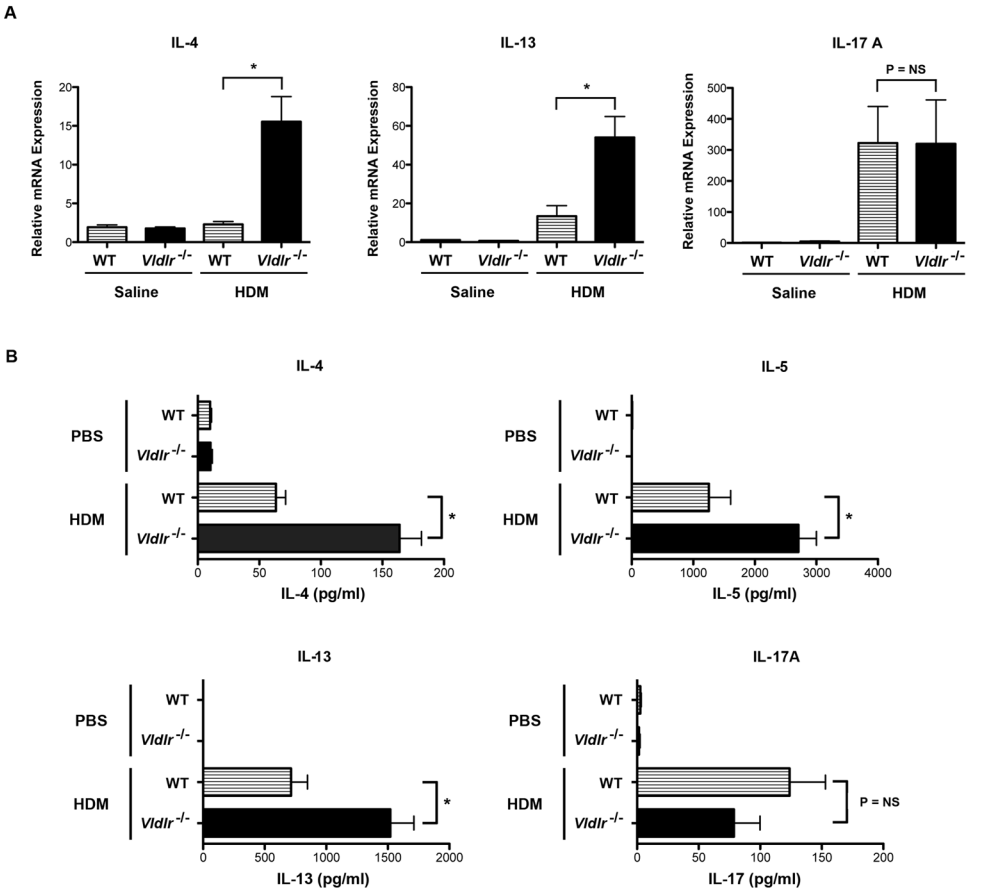

Figure 3. Th2 cytokines are increased in the lungs and mediastinal lymph nodes from house dust mite (HDM)-challenged *Vldlr*$^{-/-}$ mice

A. Quantification of lung mRNA levels by qRT-PCR for IL-4, IL-13 and IL-17A (n = 12 mice, *P < 0.0001, *Vldlr*$^{-/-}$ + HDM vs. WT + HDM). **B**. *Ex vivo* cultures of mediastinal lymph node cells from HDM-challenged *Vldlr*$^{-/-}$ and wild-type mice were re-stimulated with HDM (100 μg/ml) or PBS and the quantity of IL-4, IL-5, IL-13, and IL-17A secreted into the medium was quantified by ELISA (n = 18 – 20 mice, P < 0.0001, *Vldlr*$^{-/-}$ + HDM vs. WT + HDM).

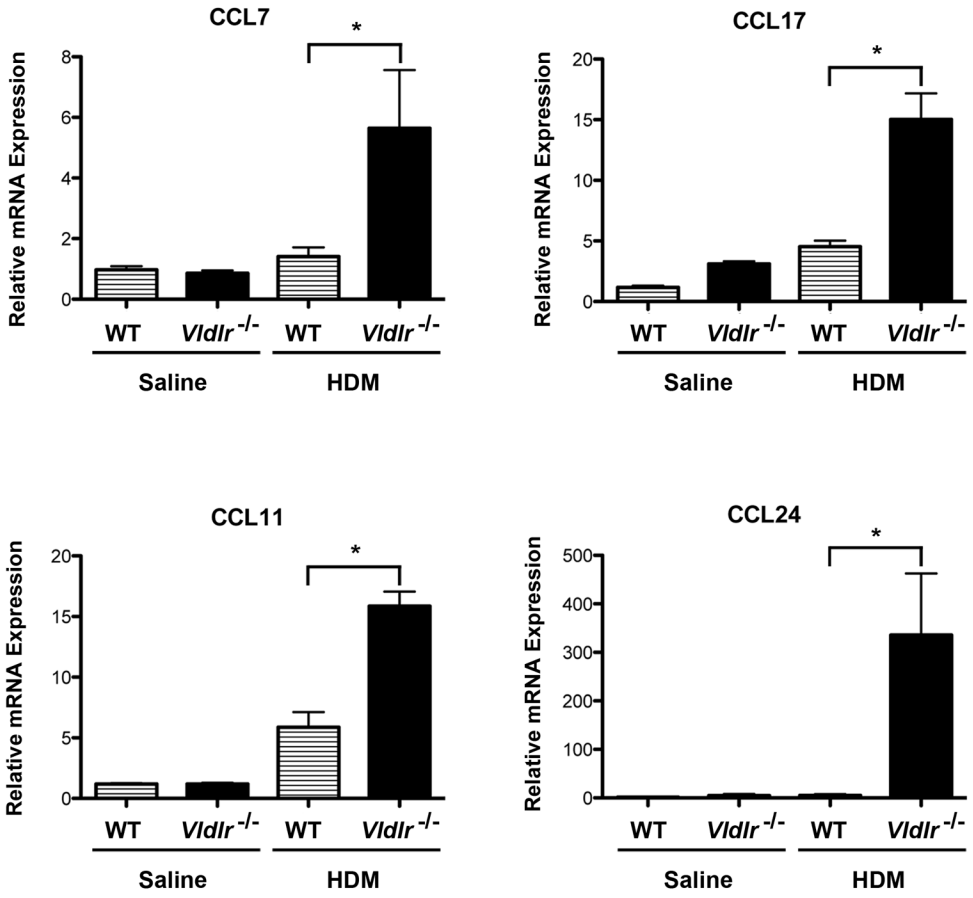

Figure 4. C-C chemokines are increased in the lungs of house dust mite (HDM)-challenged *Vldlr*$^{-/-}$ mice

Quantification of lung mRNA levels by qRT-PCR for CCL7, CCL11, CCL17 and CCL24 (n = 12 mice, *P < 0.01, *Vldlr*$^{-/-}$ + HDM vs. WT + HDM).

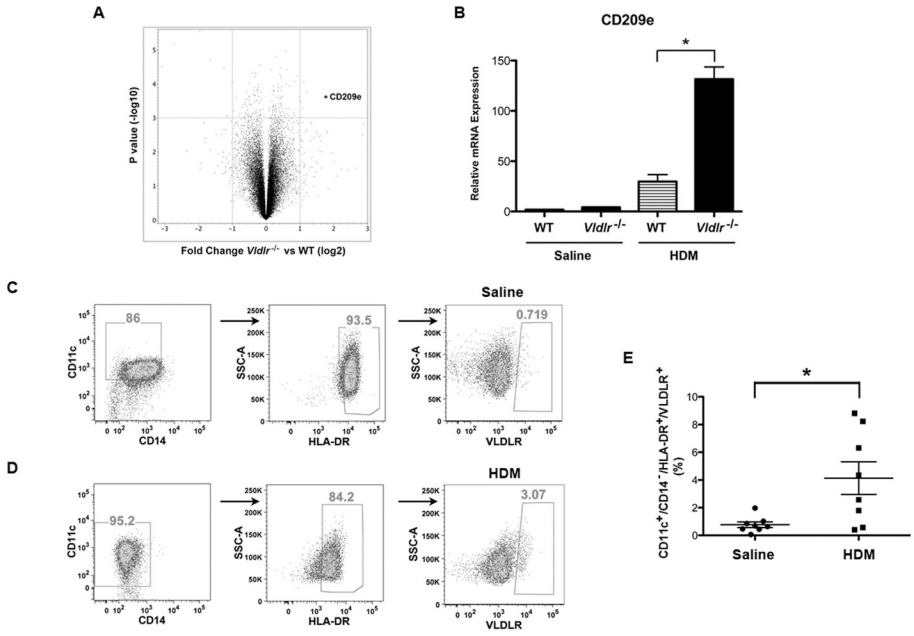

Figure 5. Genome-wide expression profiling of the lung transcriptome identifies increased expression of CD209e in house dust mite (HDM)-challenged *Vldlr*$^{-/-}$ mice

A. Volcano plot of log2 fold changes versus one-way ANOVA p-value (-log10 scale) between expressions of mRNAs isolated from the lungs of HDM-challenged *Vldlr*$^{-/-}$ and wild-type mice. Each dot represents one transcript. The cut-off for selecting differentially expressed genes were Fold Change (log2) <−1 or >1 and P value < 0.001 (FDR20%). The transcript of CD209e is indicated by an asterisk (*). **B.** Quantification of lung mRNA levels by qRT-PCR for CD209e (n = 19 – 20 mice, *P < 0.001, *Vldlr*$^{-/-}$ + HDM vs. WT + HDM). **C and D.** Representative flow cytometric analysis of human CD11c^{+}/CD14^{-}/HLA-DR^{+} bone marrow-derived dendritic cells that had been treated without (Panel C) or with (Panel D) house dust mite (100 μg/ml) for cell surface expression of VLDLR. **E**. The percentage of CD11c^{+}/CD14^{-}/MHCII^{+} human bone marrow-derived dendritic cells that express the VLDLR in response to HDM was quantified by flow cytometry (n = 8 donors, P < 0.03).

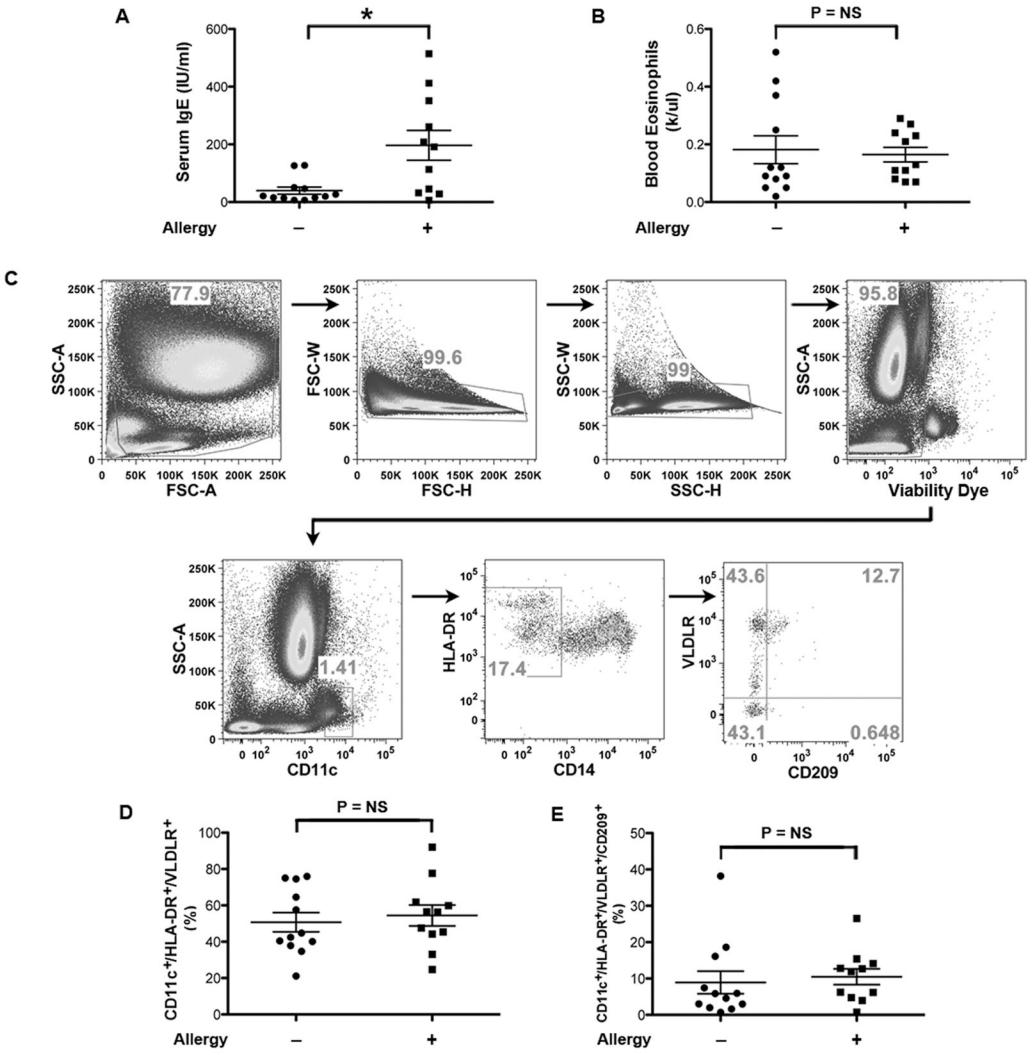

Figure 6. Characterization of cell surface VLDLR expression on peripheral blood dendritic cells from human subjects

A and B. Serum IgE levels (A) and peripheral blood eosinophil counts (B) from subjects without (n = 12) or with (n = 11) skin test reactivity to one of six common aeroallergens (* P = 0.006). **C**. Representative flow cytometric analysis of $CD11c^+/CD14^-/HLA\text{-}DR^+$ dendritic cells from peripheral blood for cell surface expression of VLDLR and CD209. Cellular debris and doublets were excluded using physical scatter properties of RBC-lysed whole blood cells and dead cells were excluded using a fixable live dead exclusion dye. Expression of VLDLR and CD209 were assessed on viable $CD11c^+/CD14^-/HLA\text{-}DR^+$ dendritic cells. **D and E.** The percentage of $CD11c^+/CD14^-/HLA\text{-}DR^+/VLDLR^+$ cells (Panel D) and $CD11c^+/CD14^-/HLA\text{-}DR^+/VLDLR^+/CD209^+$ dendritic cells (Panel E) present in peripheral blood samples from subjects without or with allergy.

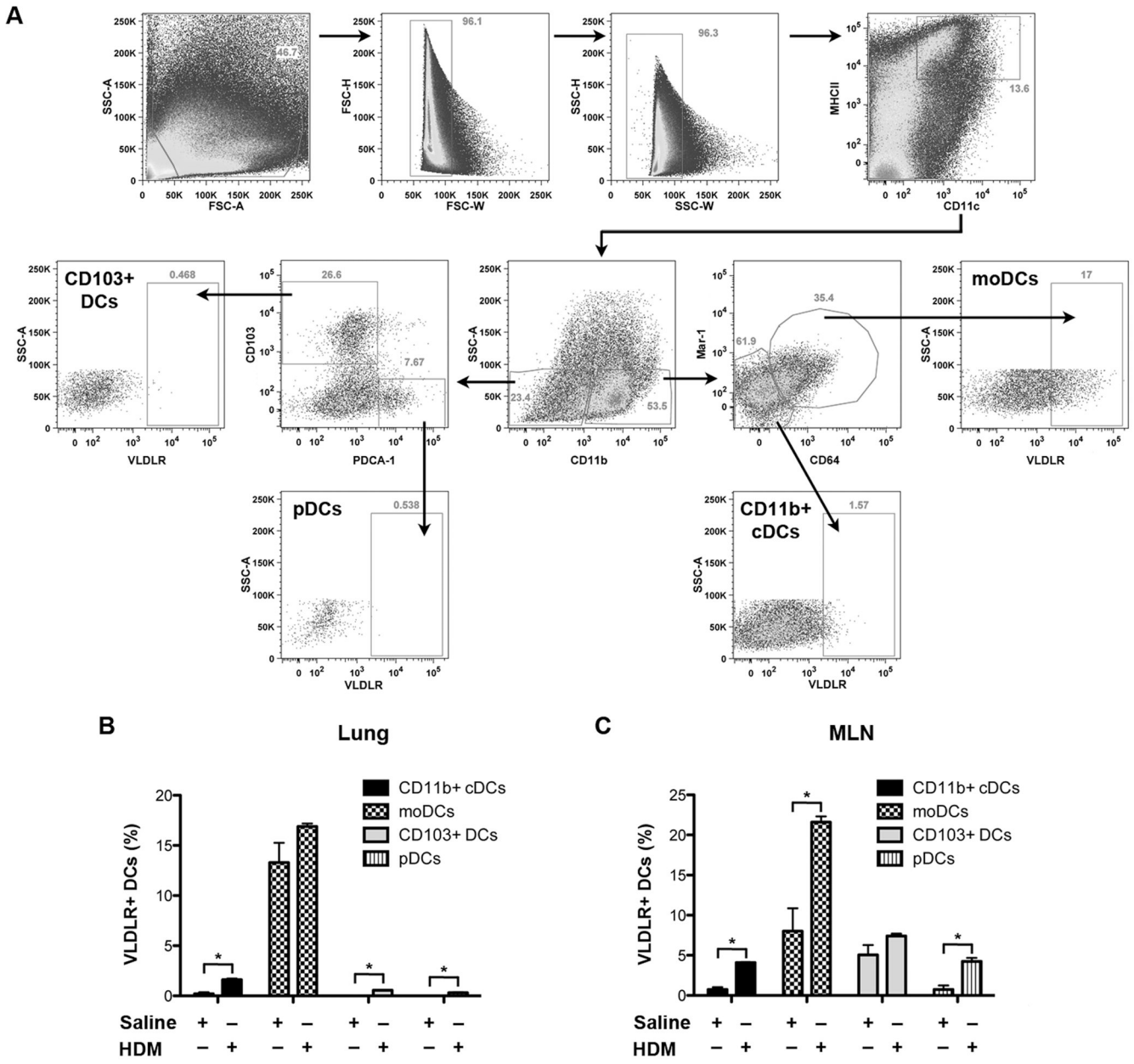

Figure 7. Characterization of cell surface VLDLR expression by dendritic cell subsets in the lungs and mediastinal lymph nodes of saline- and HDM-challenged wild type mice

A. The gating strategy utilized to analyze DC subsets present in the lung and mediastinal lymph nodes (MLN) of saline- and HDM-challenged wild type mice is presented. Cellular debris and doublets were excluded using physical scatter properties of the cells. Single $CD11c^{+}/MHCII^{hi}/SSC^{lo}$ cells from lung and MLN homogenates were included as DCs, whereas $CD11c^{+}/MHCII^{int}/SSC^{hi}$ alveolar macrophages were excluded from further analysis. DCs were gated further into $CD11b^{+}$ and $CD11b^{-}$ populations. For identification of DC subsets, $CD11b^{+}/Mar\text{-}1^{+}/CD64^{+}$ cells were classified as monocyte-derived DCs (moDCs), $CD11b^{+}/Mar\text{-}1^{-}/CD64^{-}$ cells as conventional myeloid DCs ($CD11b^{+}$ cDCs), $CD11b^{-}/CD103b^{+}$ cells as $CD103^{+}$ DCs and $CD11b^{-}/PDCA\text{-}1^{+}$ cells as plasmacytoid DCs

(pDCs)(45). A representative flow cytometric analysis of dendritic cell subsets present in the lung of a HDM-challenged wild type mouse is shown. **B**. The percentage of $VLDLR^+$ $CD11b^+$ conventional myeloid DCs ($CD11b^+$ cDCs), monocyte-derived DCs (moDCs), $CD103^+$ DCs and plasmacytoid DCs (pDCs) in the lungs of saline- and HDM-challenged wild type mice were quantified by flow cytometry (n = 9 – 10 mice, * $P \leq 0.0013$, HDM-challenged vs. saline-challenged). **C.** The percentage of $VLDLR^+$ DC subsets in the MLNs of saline- and HDM-challenged wild type mice was quantified by flow cytometry (n = 10 mice, *$P \leq 0.003$, HDM-challenged vs. saline-challenged).

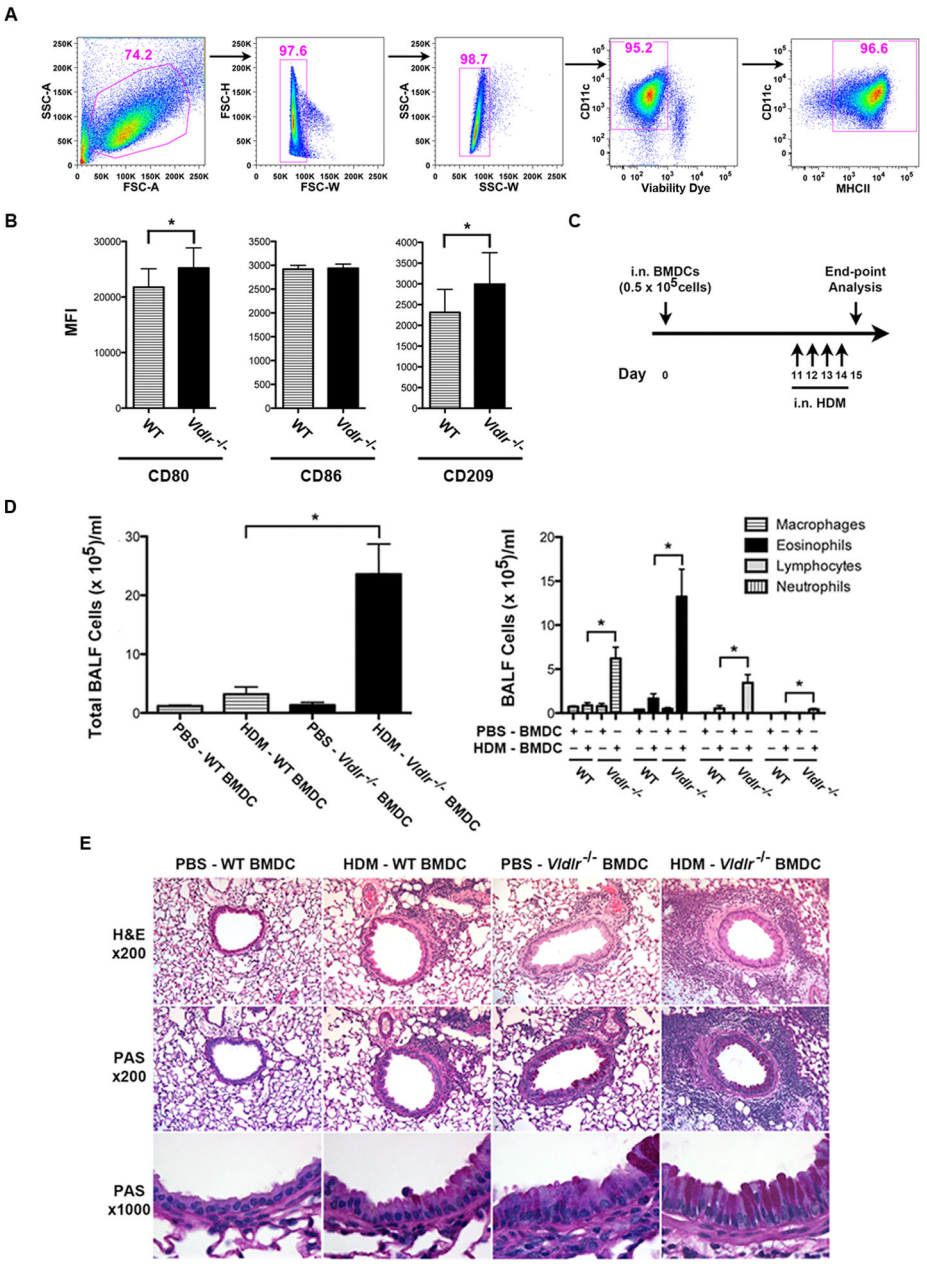

Figure 8. The adoptive transfer of HDM-pulsed, CD11c^{+} bone marrow-derived dendritic cells (BMDCs) from *Vldlr*$^{-/-}$ mice up-regulates HDM-induced airway inflammation

A. A representative flow cytometric analysis of HDM-pulsed CD11c^{+}/MHCII^{+} bone marrow-derived dendritic cells. Debris and doublets were excluded from the analysis using physical scatter properties of cells and viable CD11c^{+} cells were selected from the population of single cells using a fixable live dead exclusion dye. CD11c^{+}/MHCII^{+} cells were further analyzed for cell surface expression of CD80, CD86 and CD209 using Fluorescence minus one (FMO) as a control. **B.** MFI of cell surface expression of CD80, CD86 and CD209 by HDM-pulsed CD11c^{+}/MHCII^{+} bone marrow-derived dendritic cells. (n = 8 mice, * $P < 0.05$). Data are pooled from two independent experiments. **C.** Adoptive

dendritic cell transfer model of HDM-induced airway inflammation. On Day 0, 0.5×10^5 $CD11c^+$ BMDCs from *Vldlr*$^{-/-}$ or wild type (WT) mice that had been pulsed with HDM (HDM-BMDC) or sham-pulsed with PBS (PBS-BMDC) were adoptively transferred to recipient wild-type mice via intranasal administration. On days 11 through 14, all recipient wild type mice were challenged with HDM (30 μg/mouse) and end-points were analyzed on Day 15. **D.** The number of total bronchoalveolar (BALF) inflammatory cells and inflammatory cell types are shown. Comparisons were made between recipient wild-type mice that had received adoptive transfer of HDM-pulsed *Vldlr*$^{-/-}$ BMDCs (HDM-*Vldlr*$^{-/-}$ BMDC) versus HDM-pulsed WT BMDCs (HDM-WT BMDC) (n = 5 – 9 mice, *P < 0.01). **E.** Representative histologic sections of lungs from WT and *Vldlr*$^{-/-}$ mice that had been challenged with HDM or saline were stained with hematoxylin and eosin (H & E) (x 200) or periodic acid Schiff (x200 and x1000).

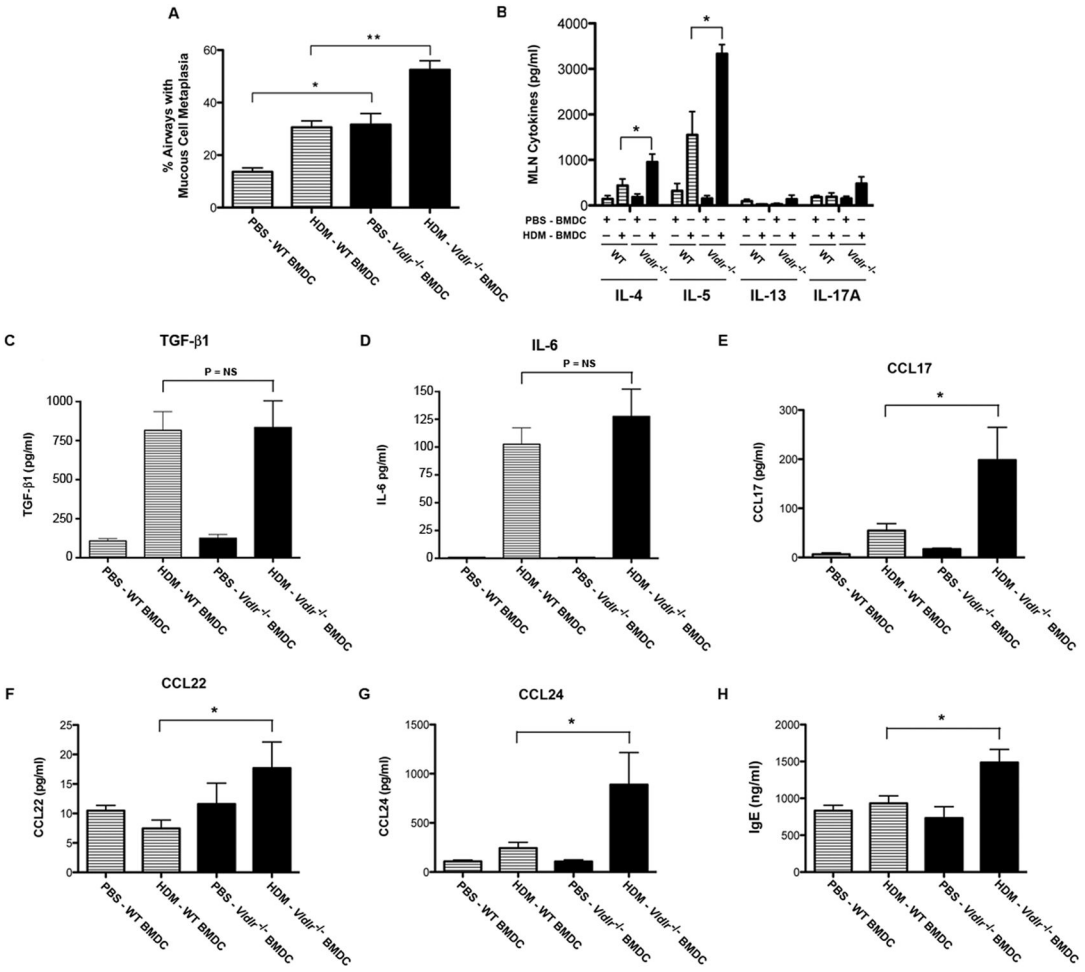

Figure 9. The adoptive transfer of HDM-pulsed, CD11c$^+$ bone marrow-derived dendritic cells (BMDCs) from *Vldlr*$^{-/-}$ mice augments the HDM-induced expression of Th2 cytokines and C-C chemokines

A. Mucous cell metaplasia is presented as the percentage of airways on lung histological sections that contained periodic acid–Schiff positive cells. Comparisons were made between HDM-challenged recipient wild-type mice that had received the adoptive transfer of HDM-pulsed, CD11c$^+$ BMDCs from *Vldlr*$^{-/-}$ versus WT donors (n = 5 – 7 mice, **P < 0.001, HDM-*Vldlr*$^{-/-}$ BMDCs vs. HDM-WT BMDCs) and PBS-pulsed, CD11c$^+$ BMDCs from *Vldlr*$^{-/-}$ versus WT donors (n = 5 – 6 mice, *P < 0.01, PBS-*Vldlr*$^{-/-}$ BMDCs vs. PBS-WT BMDCs). 13.9 ± 0.96 airways were counted per mouse. **B**. *Ex vivo* cultures of mediastinal lymph node (MLN) cells from HDM-challenged recipient wild-type mice that had received adoptive transfers of HDM-pulsed (HDM-BMDC) or sham PBS-pulsed (PBS-BMDC) CD11c$^+$ BMDCs from *Vldlr*$^{-/-}$ or wild type (WT) donors. Cultures were re-stimulated with HDM (100 μg/ml) and the quantity of IL-4, IL-5, IL-13, and IL-17A secreted into the medium was quantified by ELISA (n = 4 – 8 mice, *P < 0.05, HDM-*Vldlr*$^{-/-}$ DCs vs. HDM-WT DCs). **C – G.** Quantification of protein levels of TGF-β1, IL-6, CCL17, CCL22 and CCL24 in bronchoalveolar lavage fluid. (n = 4 – 9 mice, *P < 0.05, HDM-*Vldlr*$^{-/-}$ BMDCs

vs. HDM-WT BMDCs). **H**. Quantification of plasma IgE levels (n = 4 – 7 mice, *P < 0.01, HDM-*Vldlr*$^{-/-}$ BMDCs vs. HDM-WT BMDCs).